Some optical properties of surface waters in the north-western Tropical Atlantic

OCEANOLOGIA, No. 32
pp. 49–67, 1992.
PL ISSN 0078-3234

Tropical Atlantic
Ocean Optics
Photosynthetically
Active Radiation
Ocean Colour

Adam Krężel
Institute of Oceanography,
University of Gdańsk,
Gdynia

Marek Kamieniecki
Institute of Marine Sciences,
University of Szczecin,
Szczecin

Manuscript received March 5, 1992, in final form June 15, 1992.

Abstract

The colour of the ocean, photosynthetically active radiation (PAR) and some optical properties of the surface waters of the north-western Tropical Atlantic were measured during the cruise of r/v 'Akademik Vernadski' in June and July 1987. The superposition of the downwelling irradiance attenuation coefficients in the blue (425 nm), green (535 nm) and PAR (400–700 nm) spectral bands in the spatial distribution of optical water types in the region are presented (Fig. 5). Except for the area directly influenced by the Amazon river, the waters in the region were found to be extremely clear, *i.e.* belonging mainly to classes I to IB in Jerlov's classification.

The colour indices obtained from measurements of sea surface spectral reflectance were compared with the chlorophyll *a* concentration in the optical penetration depth layer. The low chlorophyll concentration and its small variability were probably the reason why these dependences were weak in comparison to those previously reported for Class 1 waters.

If the cloudiness does not exceed 7, the maximum possible daily PAR ranges from 1200 to 1800 $\mu Em^{-2}s^{-1}$ just under the sea surface, from 500 to 800 $\mu Em^{-2}s^{-1}$ at a depth of 10 m, and from 250 to 400 $\mu Em^{-2}s^{-1}$ at 25 m (Fig. 8).

1. Introduction

The international undersatellite experiment 'Atlantic 87' took place between 18 May and 12 August 1987 with the participation of the Ukrainian

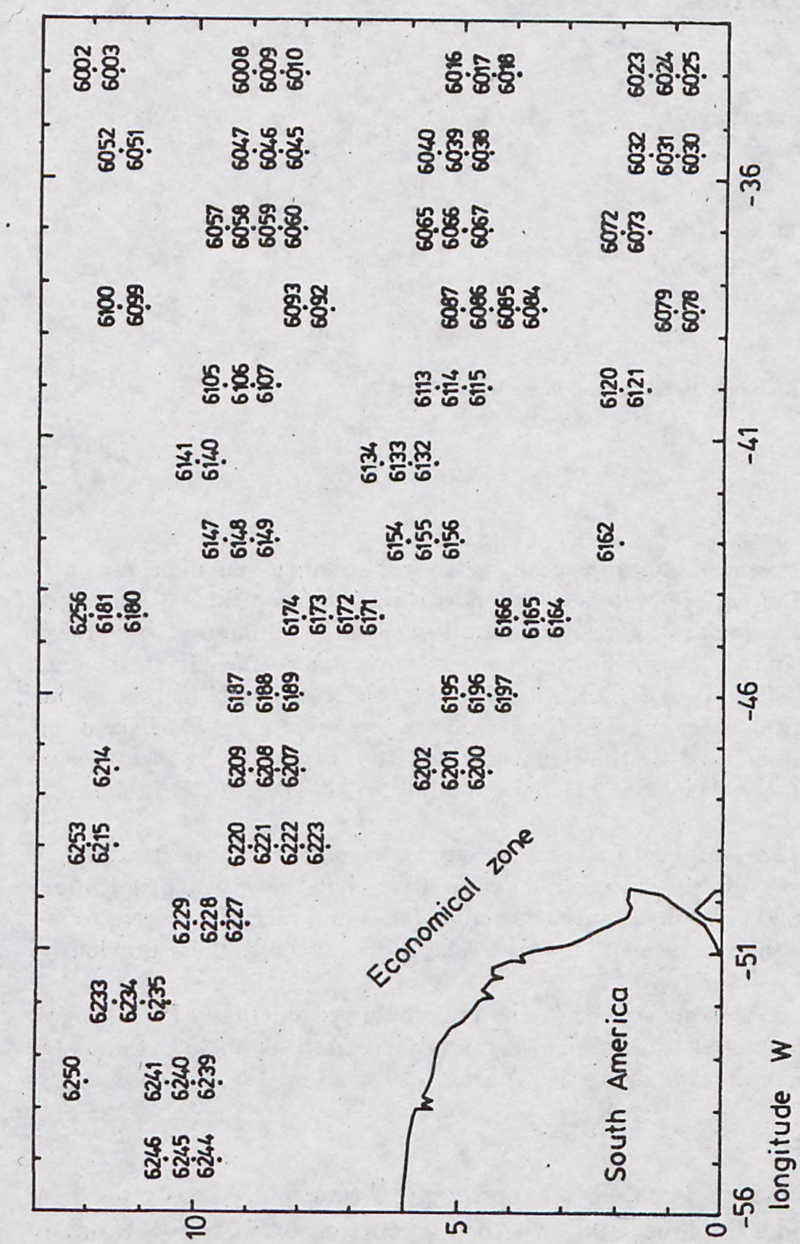

Fig. 1. Location of measuring stations

research vessel 'Akademik Vernadski' and the Russian orbital shuttle 'Salut 7'.

The aim of the experiment was to study some physical parameters of sea water using optical methods within the water and just over the sea surface in the area where clear Atlantic and Amazon waters mix.

The results were intended to be a basis for interpreting satellite-sensed material as a source of information about chlorophyll concentration in oceanic surface waters. Unfortunately, the widespread cloudiness occurring during the whole experiment made it impossible to receive even one good satellite image of the ocean surface.

The measurements were carried out within an area between longitudes 34° and 55°W, and latitudes 12°N and 0.5°S from 4 June 1978 to 21 July 1987. The positions of the measuring stations are shown in Figure 1.

The nature of the measured parameters required the investigations to be carried out only during the daytime, *i.e.* under appropriate light conditions. The Polish team made measurements at 120 of the 262 measuring stations.

The following parameters were measured at every station: the sea surface albedo in 16 spectral bands, the absolute downwelling irradiance in the photosynthetically active part of the solar spectrum (PAR), and the relative downwelling irradiance in the 425 and 535 nm spectral bands[1]. The last two parameters were measured down to a depth of 30 m (the technically feasible depth).

2. Oceanographical characteristics of the investigated area

The area of investigation as defined by Terziev *et al.* (1986) lies within the Energy-active Zone of the Tropical Atlantic (EZTA). The main climatological features giving rise to physical processes in this part of the ocean are the trade winds and the positive radiation budget. Both strongly influence the thermodynamics of the surface water layer. The mean annual wind speed ranges from 6 to 10 $\mathrm{m \cdot s^{-1}}$, the prevailing directions being NE and E. In June and July the winds are slightly weaker (75% from 3 to 5 $\mathrm{m \cdot s^{-1}}$). It is a region of high precipitation ($\leq$ 3000 mm annually), high humidity ($>$ 80%) and considerable cloudiness. The cloud cover is 70–100% for 50% of the year.

The thermodynamic fields in the upper ocean layer are quasi-stationary. The water temperature ranges between 25° and 28°C, the salinity between 35.5 and 36.2 psu. The greater ranges and gradients occur only within a belt along the South American coast and are directly connected with the

[1]All the optical values used in the paper are in accordance with the ones used by Dera (1992).

inflow of Amazon water. The influence of the Amazon River is particularly evident within the shelf area and surface layer down to 15–20 m (Terziev *et al.*, 1986). Outside the shelf area but inside the EZTA region there is rather weak convectional mixing. Wind-generated mixing reaches depths of 60–70 m and the thermocline occurs at depths of 100 to 140 m.

The South Equatorial Current, the Equatorial Countercurrent, and the North Brazil and Guyana Currents are the main components of the surface circulation in the region. The last of these has a particularly strong influence on the mixing of Amazon and oceanic waters, carrying the former northwards up to 1000 km from the river mouth (Bowden, 1983; Cadée, 1975). Of great importance to heat transport within the investigated area is the quasi-stationary anticyclone, centred at latitude 5°N and longitude 42°–44°W. The heat transport is the result of small, hot anticyclones escaping from this main vortex and migrating further northwards with the Guyana Current (Terziev *et al.*, 1986).

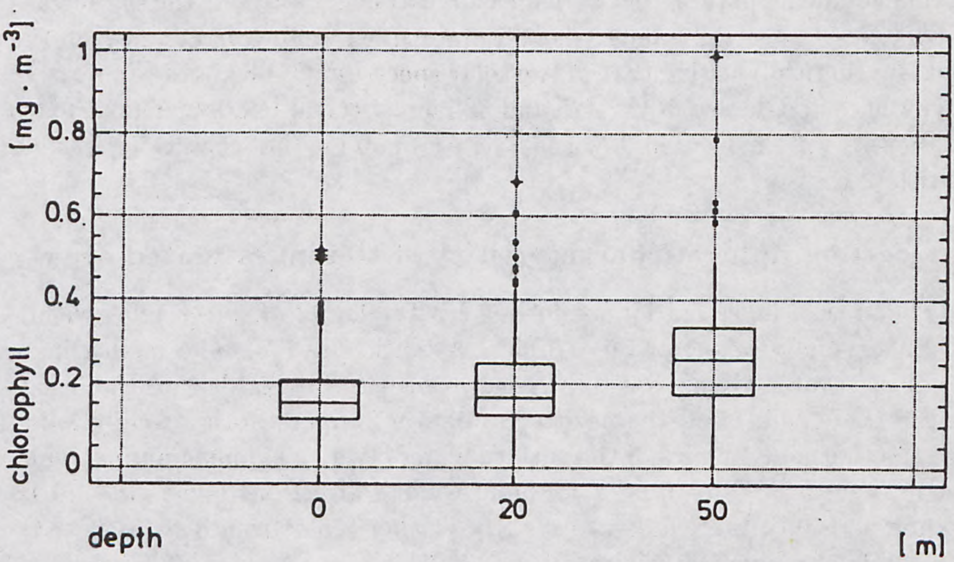

Fig. 2. Statistics[2] of chlorophyll *a* concentration in the surface waters of the north-western Tropical Atlantic in June and July 1987

---

[2] John Tukey's (1981) 'Box-and-Whisker' Plot. The central boxes cover the middle 50% of the data values, between the lower and upper quartiles. The 'whiskers' extend out to the extremes, while the central line is at the medium. The whiskers extend only to those points that are within 1.5 times the interquartile range. The outlier values are plotted as separate points.

Primary production in EZTA waters is said to be among the lowest in the World Ocean. According to Raymont (1983), the daily primary production here ranges from *ca* 100 to 150 $\mathrm{mg\,C \cdot m^{-2}}$. Cadée (1975) shows that it can be even lower than 100 $\mathrm{mg\,C \cdot m^{-2}}$. On the other hand, Koblentz-Mishke (Oceanobiologia..., 1988) points out the possible occurrence of local patches connected with cooler cyclonic eddies where the daily primary production exceeds 250 $\mathrm{mg\,C \cdot m^{-2}}$. The distribution of chlorophyll concentration obtained from satellite data (CZCS radiometer) shows that it does not exceed 0.15 $\mathrm{mg \cdot m^{-2}}$ in the study area. At some places it decreases below 0.05 $\mathrm{mg \cdot m^{-2}}$, *i.e.* to the value characteristic of the Sargasso Sea, which is known as 'the sea desert' (Ocean Color (1989)). Figure 2 shows the main statistical characteristics of chlorophyll concentration in the ocean at depths of 0, 20 and 50 m obtained during the expedition. Clearly, these are rather larger than those cited above.

3. Measurements of the sea surface albedo

Simultaneous measurements of the downwelling irradiance E_d and upwelling radiance L_u in 16 spectral bands between 436 and 1000 nm were carried out. Consecutive spectral intervals were cut off by interference filters with a half-width of *ca* 10 nm. The device was suspended about 5 m over the sea surface on the sunny side of the ship. Every measurement consisted of 10 to 25 single sensings. After filtering the values exceeding ± 0.5 of the standard deviation (to eliminate sun glitter), the results were used to calculate the sea surface albedo.

The spectroalbedometer, which enabled absolute values of E_d and L_u to be obtained, was calibrated in a few steps. The calibration data from the 'Black Sea 85' experiment,[3] obtained in the laboratory, and the downwelling irradiance measured under ideal atmospheric conditions at some measuring stations during the expedition were used. The downwelling irradiance measured under a clear sky were compared with those calculated using Bird and Riordan's (1986) spectral model for irradiance at the Earth's surface for a cloudless atmosphere – SPECTRAL 2.

Table 1 shows some measurements made at one of the measuring stations, after filtering and calibration.

The sea surface reflectance (ρ_s) was calculated from

$$\rho_s = \frac{\pi L_u(\lambda)}{E_d(\lambda)}. \qquad (1)$$

[3]During the expedition on the Black Sea, the spectroalbedometer was calibrated against the German MKS spectrometer described by Sümnich (1987).

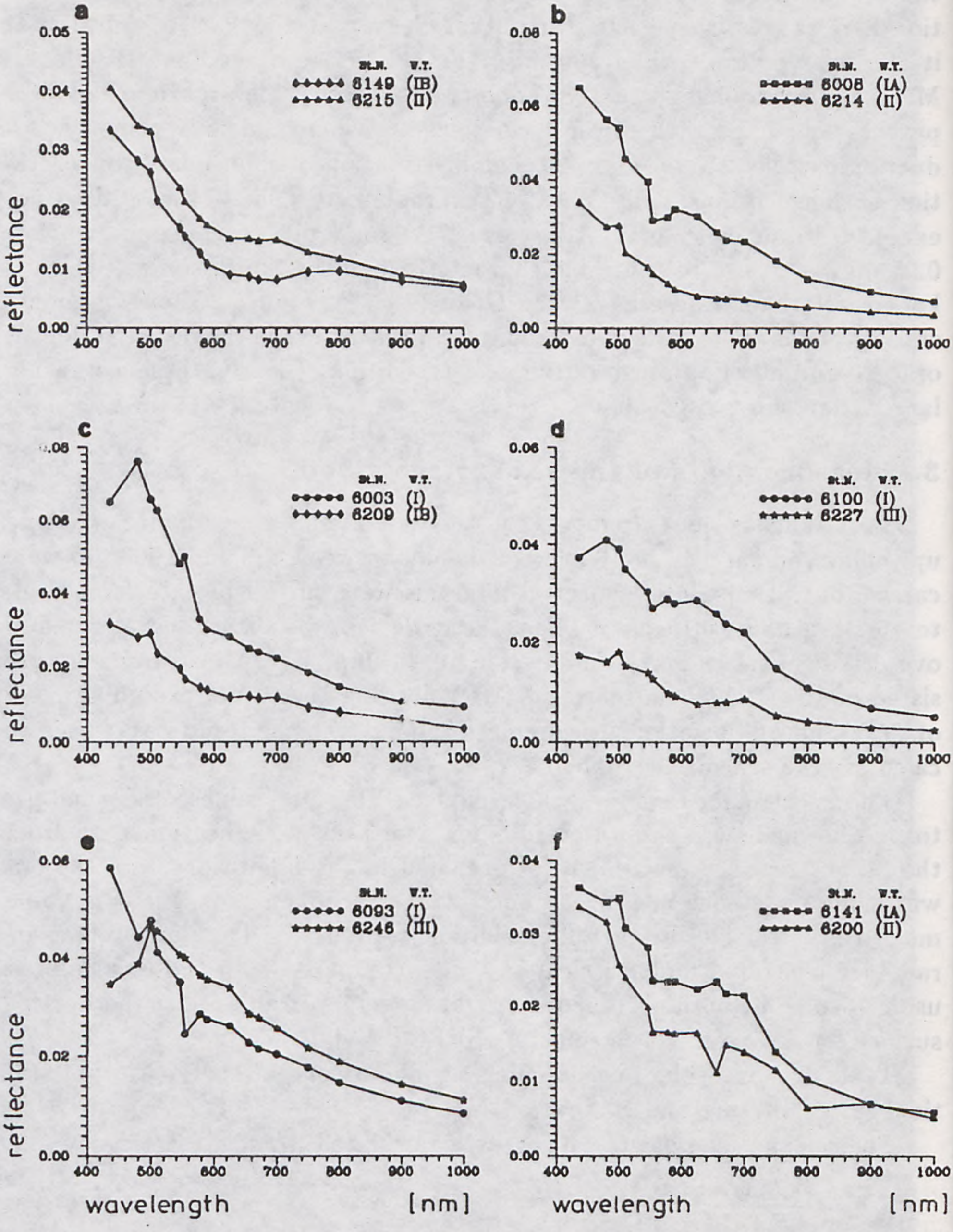

Fig. 3. Examples of sea surface reflectance spectra ρ_s (eq. 1) for different environmental conditions (St. N. – station number, W. T. – Jerlov's water type)

	cloudiness				solar zenith distance		
a	≤2	d	2–7	a	<40°	d	<80°
b	≤2	e	<7	b	>80°	e	<40°
c	2–7	f	>7	c	<40°	f	>80°

Table 1. Examples of optical measurements over the sea surface at station No. 6099; Date: 18 June 1987; Time: 11:45 GMT; Latitude: 11°00'N; Longitude: 38°30'W; Solar Zenith Distance: 40°00'; Sea state (Beaufort scale): 4; Cloudiness (tenths): 0.7;
Colour Indices: J(436, 546): 1.665; J(436, 554): 2.026; J(480, 546): 1.464; J(480, 554): 1.782

No.	λ	L_u	E_D	ρ_s
.	[nm]	[μWcm^{-2}nm^{-1}sr^{-1}]	[μWcm^{-2}nm^{-1}]	
1	436	0.4322	34.7499	0.03907
2	480	0.4497	41.1159	0.03436
3	500	0.4298	38.8495	0.03475
4	510	0.3450	41.6451	0.02603
5	546	0.3008	40.2619	0.02347
6	554	0.2483	40.4463	0.01928
7	578	0.1902	29.9187	0.01997
8	589	0.1849	28.6003	0.02031
9	625	0.1667	26.6074	0.01968
10	656	0.1710	29.8489	0.01800
11	671	0.1544	28.2741	0.01715
12	700	0.1604	29.5618	0.01704
13	750	0.0802	19.9892	0.01261
14	800	0.0591	18.9163	0.00982
15	900	0.0221	9.9946	0.00696
16	1000	0.0219	12.9251	0.00533

Examples of spectra of these reflectances under different environmental conditions are shown in Figure 3.

Table 1 additionally gives the colour indices J(436, 546), J(436, 554), J(480, 546) and J(480, 554) calculated from the formula

$$J(\lambda_1, \lambda_2) = \frac{\rho_s(\lambda_1)}{\rho_s(\lambda_2)}. \tag{2}$$

Because of the rather complicated and not very precise calibration procedure, the error inherent in the determination of L_u and E_d was estimated at about 15%; in the case of very low values, this could be even greater. Moreover, the limited capabilities of the measuring device made a reliable calculation of L_u just under the sea surface impossible. This is probably one more source of error in determining the colour index dependence on chlorophyll concentration in sea water. The preliminary measurements, examples of which are shown in Table 1, were used for further analysis. Its aim was to find the dependence of the appropriate colour indices on chlorophyll concentration in the surface layer of the ocean, as well as on other optical parameters determined within this layer. The sea state, cloudiness, time of measurement *etc.* were also included in this analysis.

4. Underwater measurements

It is accepted (Gordon, McCluney, 1975) that the thickness of the water layer from where the optical signal sensed at the satellite level originates is approximately the inverse of the downwelling irradiance attenuation coefficient K_d. Known as the penetration depth, it is denoted by z_{90}.[4] This is why the downwelling irradiance within the surface layer was measured at the same time as its spectral optical characteristics.

Two measuring devices were used – an irradiance meter enabling the relative downwelling irradiance in two spectral bands of 425 and 535 nm to be measured, and a quanta meter for measuring PAR. The measurements were made in approximately stable light conditions at 5 m depth intervals. The downwelling irradiance attenuation coefficient was calculated from

$$K_d = -\frac{1}{\Delta z}\frac{\ln E_d(z_1)}{\ln E_d(z_2)}, \tag{3}$$

where

z_1 and z_2 – denote two different depths, obtained from the definition of this coefficient, *i.e.*

$$K_d = -\frac{1}{E_d}\frac{dE_d}{dz}. \tag{4}$$

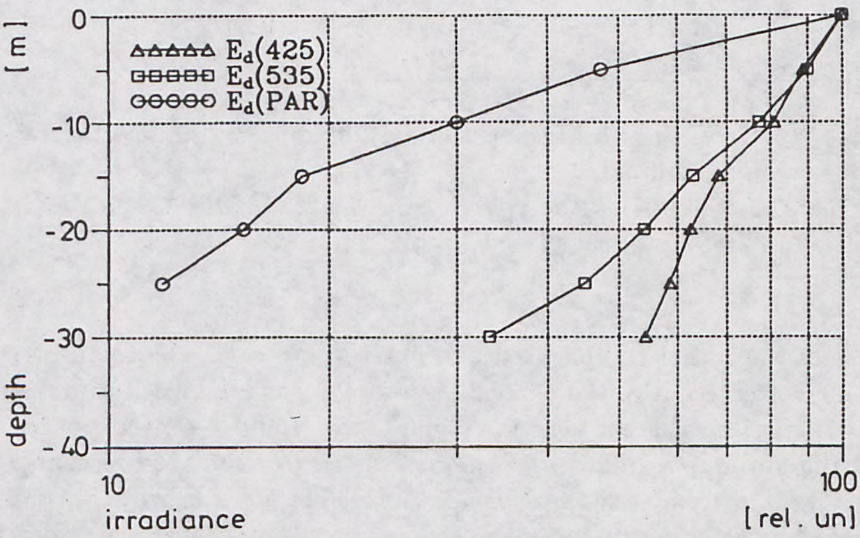

Fig. 4. Depth profiles of downwelling irradiance in the blue (425 nm), green (535 nm) and PAR spectral bands at station No. 6017

[4]About 90% of the diffusely reflected radiance leaving the sea surface originates within the layer of the first optical attenuation length (Gordon, McCluney, 1975).

The mean coefficients of K_d within the 0–10 and 10–30 m layers were calculated using the least square method. These layers were adopted after analysis of the results, which were relatively uniform there. The maximum depth of measurements was limited by the length of the measuring cable.

Figure 4 shows examples of the vertical distribution of the downwelling irradiance in the 425, 535 nm and PAR spectral bands measured at station No. 6017. The PAR values obtained were used to calculate the depth of the euphotic zone. This parameter too is within the orbit of interest of remote sensing methods (Gordon, Morel, 1983).

5. The optical classification of the north-western Tropical Atlantic

The spatial distributions of optical types of water (Fig. 5)[5] and of the depth of the euphotic zone (Fig. 6) were prepared from the calculated $K_d(425)$, $K_d(535)$ and $K_d(\mathrm{PAR})$ coefficients.

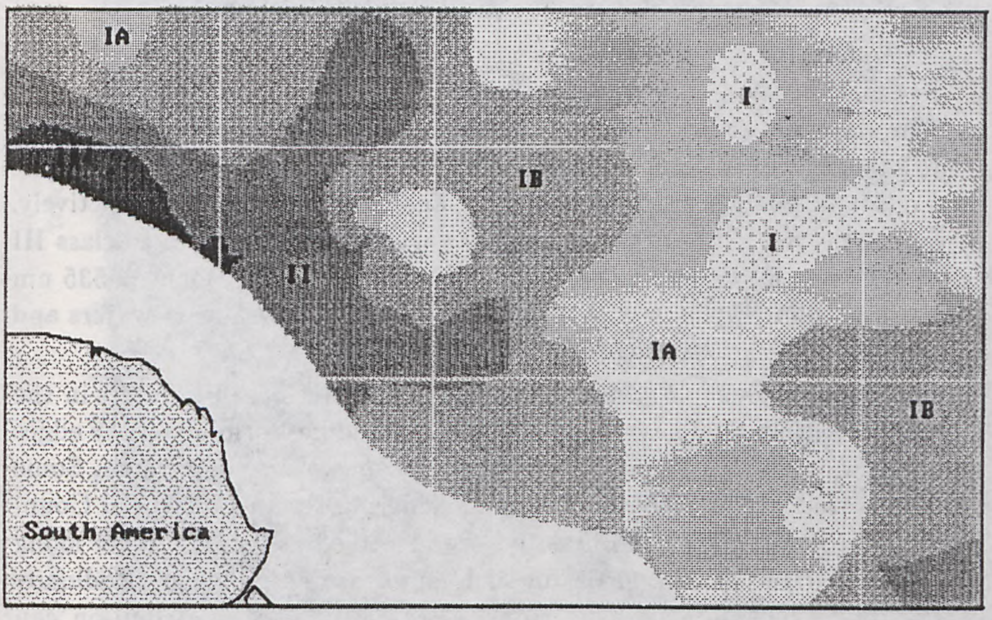

Fig. 5. Distribution of optical water types in the north-western Tropical Atlantic

[5] according to Jerlov's classification (Jerlov, 1976).

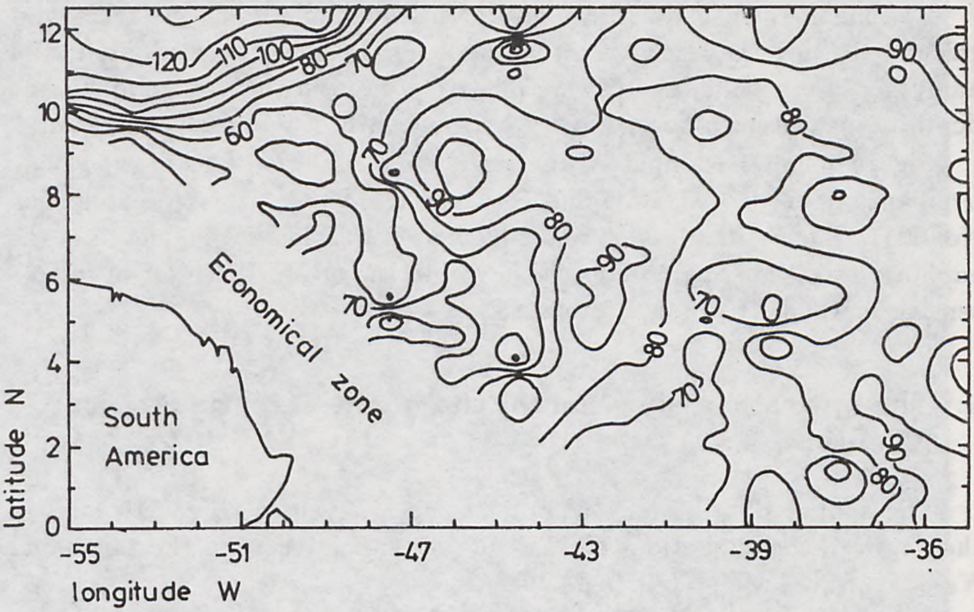

Fig. 6. The depth of the euphotic zone [m] in the north-western Tropical Atlantic

The waters of the eastern part of the investigated area belong to classes from I to IB, *i.e.* with $K_d(425)$, $K_d(535)$ and $K_d(\mathrm{PAR})$ lying within the intervals 0.021–0.06 m^{-1}, 0.043–0.07 m^{-1} and 0.045–0.075 m^{-1} respectively. In the north-western part of the area, the water type decreases to class III or even 1 (*i.e.* $K_d = 0.25$ m $^{-1}$ for $\lambda = 425$ nm, 0.14 m^{-1} for $\lambda = 535$ nm and 0.20 m^{-1} for PAR). Owing to the participation of Amazon waters and to the nature of the water circulation in the area.

Waters with higher K_d values intrude into clearer oceanic waters in the form of embayments. These are caused by small eddies forming on the edges of the Guyana Current which transports Amazon waters northwards. Some of these waters are intercepted by the meandering North-Equatorial Countercurrent (Schott, Böning, 1991) and are identified as lenses further along its route. The optical properties of such lenses are described by Rodionov *et al.* (1986). These general features of water 'quality' distribution can also be gleaned from the summer maps of surface water salinity in this area (Rühle and Zalewski (eds.), 1982).

The histograms in Figure 7 illustrate the predominance of highest optical purity waters over lower-class waters within the area under investigation in summer 1987.

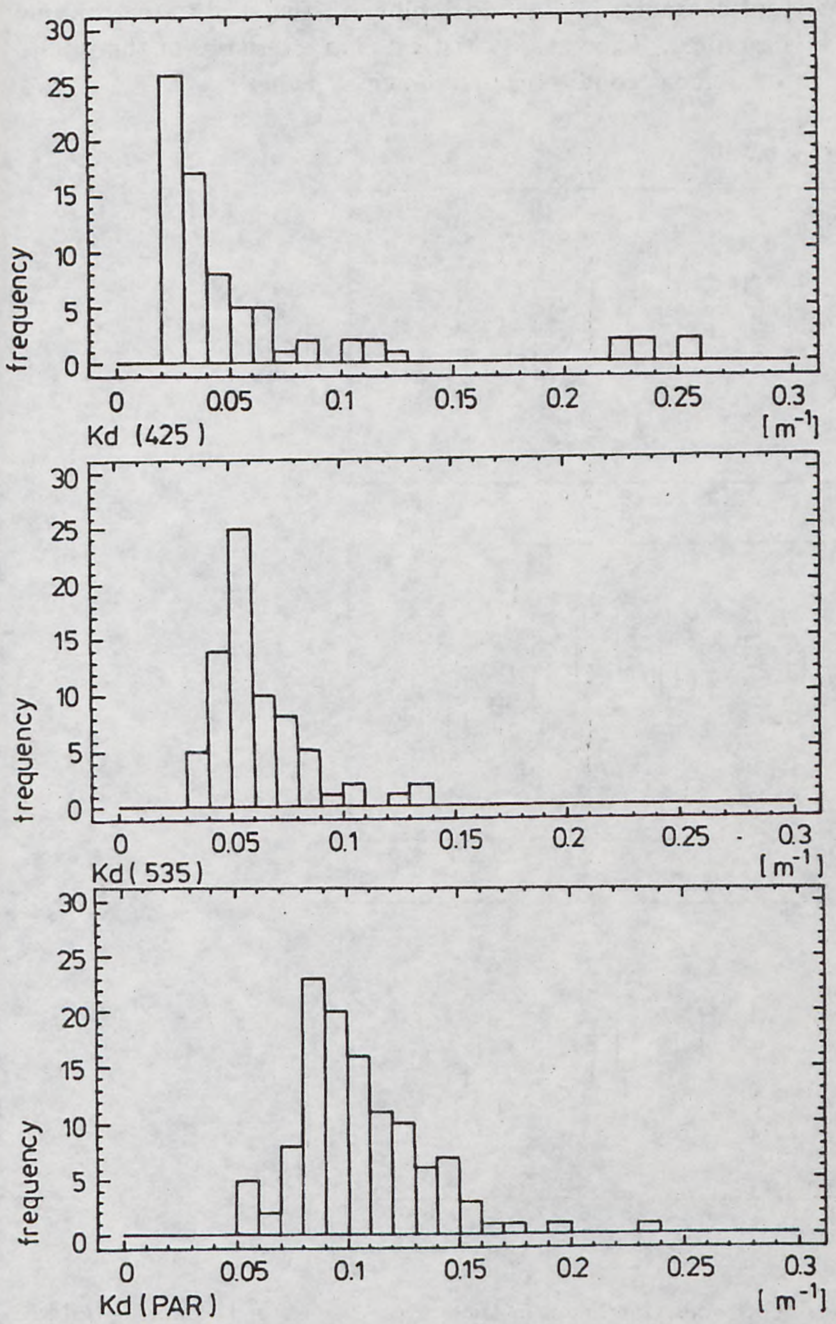

Fig. 7. $K_d(\lambda)$ coefficients in the surface waters of the north-western Tropical Atlantic in June and July 1987

6. Photosynthetically Active Radiation

The results of about 130 vertical soundings with the quantameter enabled the range and character of PAR variability in the study area in June and July to be described. The basic statistical characteristics of this radiation and the measurement conditions are shown in Table 2.

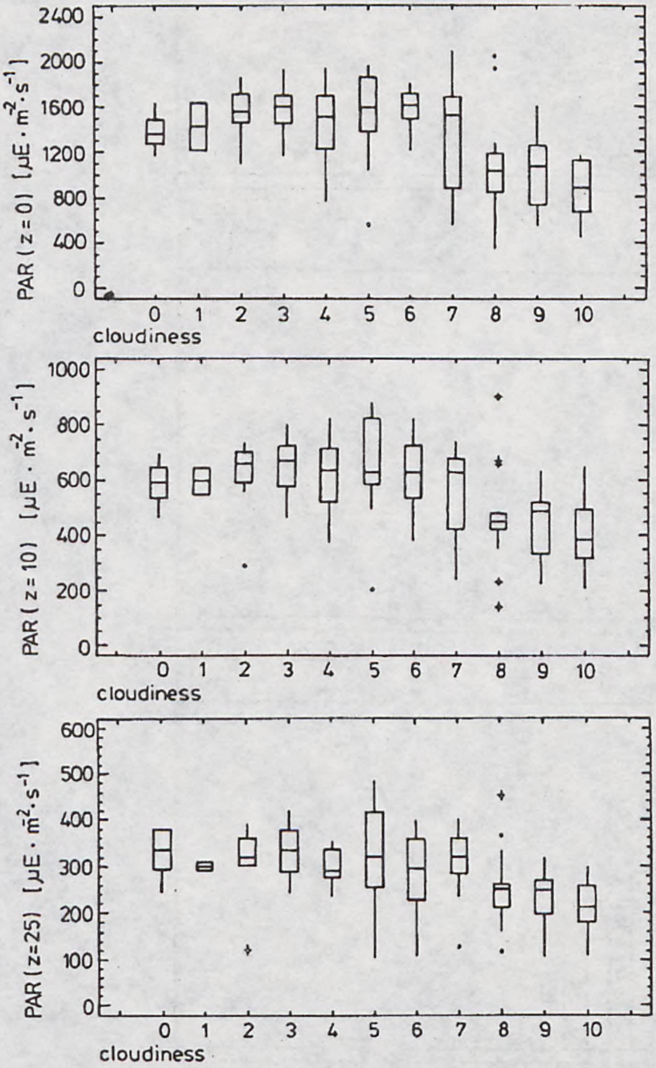

Fig. 8. PAR *vs* depth and cloudiness in the surface waters of the north-western Tropical Atlantic in June and July 1987

Table 2. Photosynthetically Active Radiation in the north-western Tropical Atlantic

Variable	0 oss	0 uss	10 m	25 m	SZD	Cloud.
Sample size	128	128	128	125	128	128
Average	939	709	280	138	40.6	6
Median	838	646	23	116	36.2	7
Mode	1650	1265	275	176	29.6	10
Standard deviation	642	489	204	102	18.3	3
Minimum value	44	37	9	4.3	9.9	0
Maximum value	2750	1705	715	396	77.8	10
Range	2706	1668	706	392	69.9	10

where
PAR – in [$mEm^{-2}s^{-1}$] over (0 oss) and under (0 uss) sea surface, and at depths of 10 and 25 m,
SZD – solar zenith distance in [deg],
Cloud. – cloudiness on a 0 – 10 scale.

The graphs in Figure 8 illustrate PAR variability versus cloudiness and depth. It was possible to compare the measurements made at different times of the day, *i.e.* at different solar elevations, in that all the values were reduced to those fulfilling the SZD = 0 condition. The dependence on cloudiness decreases with increasing depth. PAR values decrease rapidly when <70% of the sky is cloudy. This is due mainly to the decreasing probability that direct solar radiation will reach the sea surface.

7. Optical penetration depth in the 425 and 535 nm bands

The spatial distributions of the optical penetration depth were obtained from the results of $K_d(\lambda)$ calculations. These distributions for wavelengths of 425 and 535 nm are shown in Figures 9 and 10. As mentioned earlier, the signal reaching the sensor above the sea surface originates within the layer from 0 to z_{90} m. Accordingly, the distributions in Figures 9 and 10 show the depth of the layer where the parameters whose characteristics are to be determined remotely ought to be measured. In the study area this is the surface layer down to 50 m for the 'blue 'and 25 m for 'green ' spectral channel.

8. Relationships between some physical properties of sea water and colour indices

The chlorophyll a concentration and the total beam attenuation coefficient $c(420\ \mathrm{nm})$ were the other measured parameters which could be of interest from the remote sensing point of view.

Chlorophyll was measured at depths of 0, 20 and 50 m. This enabled the so-called equivalent concentration C_s within the surface layer down to a depth of z_{90} m to be calculated under certain limiting conditions. According to Gordon and Clark (1980) and Sathyendranath and Platt (1989), when the pigment, C(z) is not uniformly distributed within the optical penetration layer, the effective signal sensed by the upwelling radiance meter is equal to that originating within a similar layer with a uniform pigment distribution C_s defined by

$$C_s(\lambda) = \frac{\int_0^{z_{90}(\lambda)} C(z) f(z) dz}{\int_0^{z_{90}(\lambda)} f(z) dz}, \tag{5}$$

where

$$f(z) = \exp\left[-\int_0^z 2K_d(\lambda, z')dz'\right]. \tag{6}$$

In order to find the relationships between the colour indices and the chlorophyll a concentration, the values of C_s, calculated according to Gordon's model, have been used. I was assumed that $K_d(\lambda) = \mathrm{const}$, and the chlorophyll a concentration varied linearly between the measuring depths.

In order to eliminate certain events disturbing the $C_s = f[J(\lambda_1, \lambda_2)]$ relationship, the dependence of the colour indices on the solar zenith distance (SZD) was examined. It was found that if $\lambda_1 > \lambda_2$, then the value of $J(\lambda_1, \lambda_2)$ decreased with increasing SZD. Making allowance for that caused the correlation coefficient between C_s and $J(\lambda_1, \lambda_2)$ to increase by about 0.1.

A dependence between chlorophyll concentration in the surface layer of the ocean and the colour indices J(546, 436), J(554, 436), J(546, 480) and J(554, 480) was sought on the basis of Gordon and Morel's (1983) classic formula

$$C_s = aJ(\lambda_1, \lambda_2)^b, \tag{7}$$

which includes the above mentioned dependence of $J(\lambda_1, \lambda_2)$ on SZD. Only those events when the Sun was seen and the solar zenith distance did not exceed 80° were taken into account. The results of regression analysis are shown in Table 3.

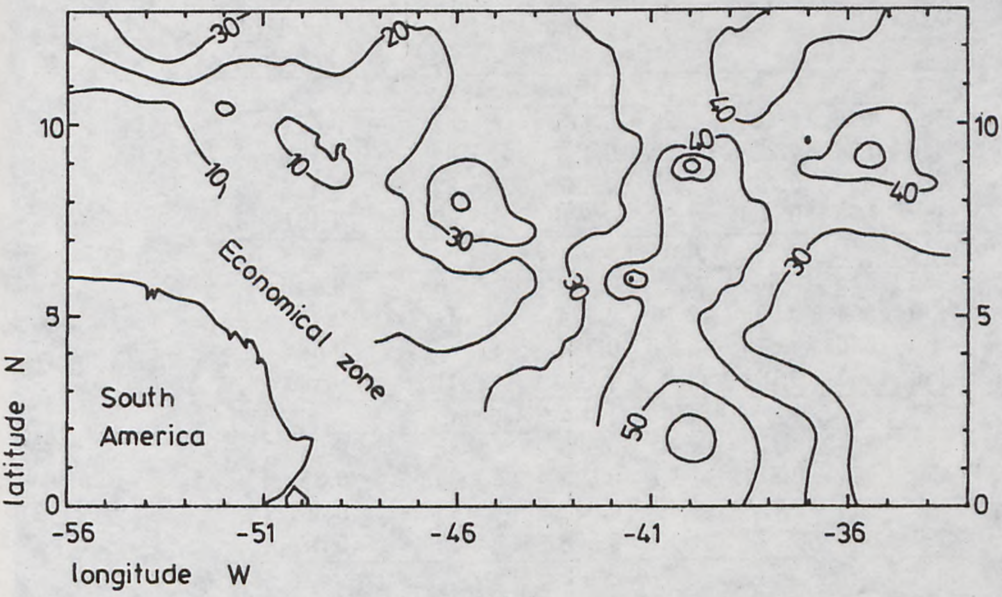

Fig. 9. The optical penetration depth z_{90} [m] in the blue (425 nm) spectral band

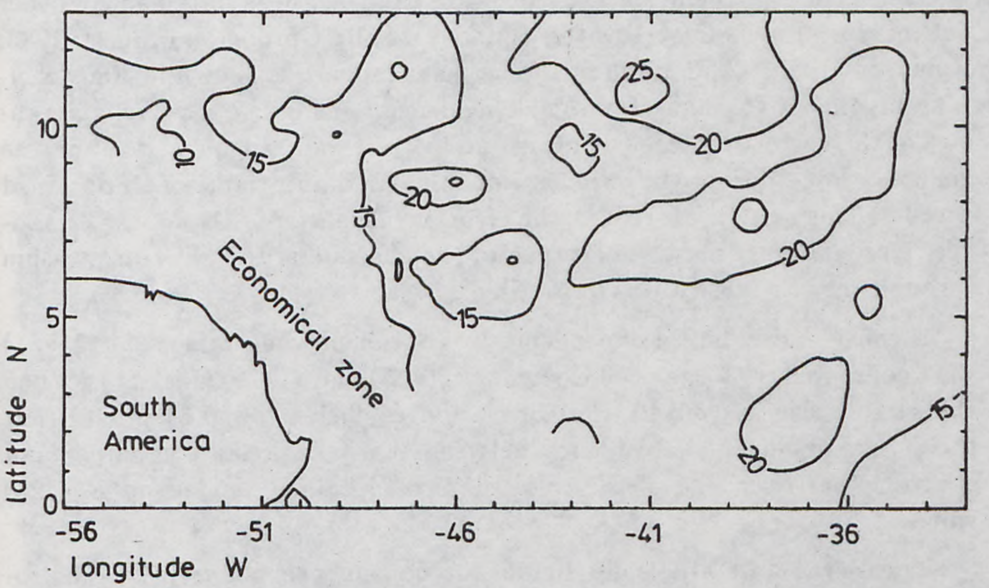

Fig. 10. The optical penetration depth z_{90} [m] in the green (535 nm) spectral band

Table 3. Coefficients of equation (7) and parameters describing the strength of this relationship

λ_1	λ_2	a	b	correlation coefficient	sample size	standard deviation
			$C_s[\mathrm{mgm}^{-3}] = aJ(\lambda_1, \lambda_2)^b$			
436	546	0.225	-1.24	0.413	32	0.441
436	554	0.278	-1.22	0.454	32	0.431
480	546	0.242	-1.45	0.427	32	0.437
480	554	0.303	-1.39	0.470	32	0.427
			$K_d[\mathrm{m}^{-1}] = aJ(\lambda_1, \lambda_2)^b$			
436	546	0.064	-2.82	0.660	56	0.541
436	554	0.095	-2.76	0.774	41	0.433
480	546	0.073	-3.04	0.584	56	0.584
480	554	0.104	-2.75	0.664	41	0.484
			$c(420)[\mathrm{m}^{-1}] = aJ(\lambda_1, \lambda_2)^b$			
436	546	0.752	-1.40	0.593	85	0.347
436	554	0.874	-1.10	0.573	85	0.353
480	546	0.798	-1.48	0.522	85	0.367
480	554	0.898	-1.10	0.508	85	0.371

The differences between particular relationships are clearly not too big, and the values of coefficients a and b are close to those obtained by other authors for Morel's Case 1 waters (quoted *e.g.* by Gordon and Morel, 1983; Robinson, 1985). The graph of the best dependence is shown in Figure 11. It seems that the weakness of this dependence, seen in the relatively low values of the correlation coefficient, is due to the small range interval and the generally low chlorophyll concentration (the maximum value of C_s obtained was 0.415 $\mathrm{mg \cdot m^{-3}}$). Moreover, the error in calculating $J(\lambda_1, \lambda_2)$ was relatively large, because accurate filtering of the effects due to light transmission through the sea surface was impossible.

A considerably better dependence was obtained when values of $J(\lambda_1, \lambda_2)$ were compared with the coefficients of $K_d(425)$ and $c(420)$ (Fig. 11). When the sample size is over 40, the correlation coefficient of -0.74 proves that there is a significant dependence between the parameters compared, and suggests that over 50% of the colour indices obtained depend on $K_d(425)$ values.

There was no statistically significant dependence between the chlorophyll *a* concentration and the values of the $c(420)$ and $K_d(425)$ coefficients.

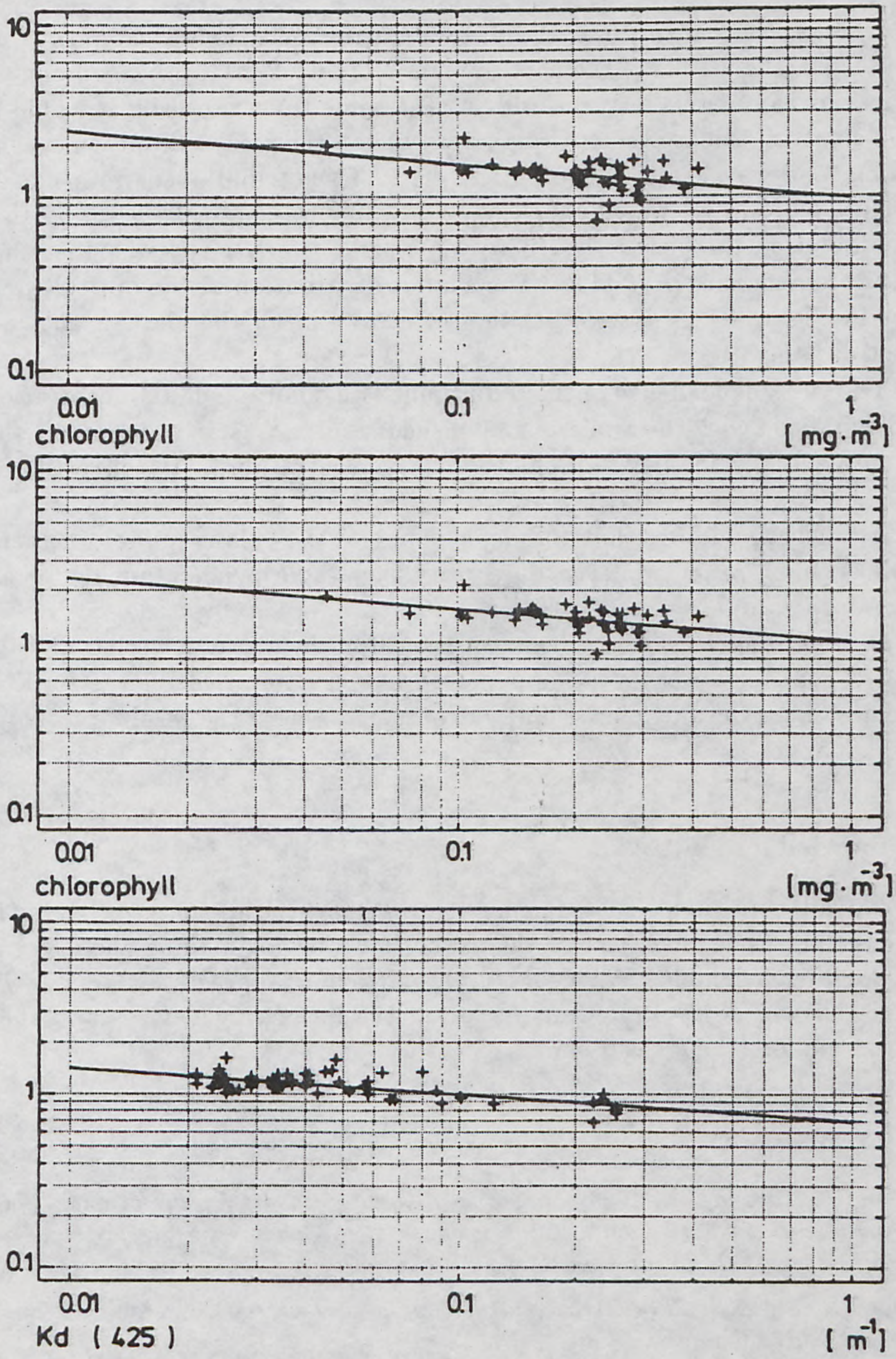

Fig. 11. Regression of chlorophyll *a* and $K_d(425)$ data *vs.* colour indices in the north-western Tropical Atlantic in June and July

9. Concluding remarks

The results confirm that, except for a narrow belt along the South American shelf, the waters of the north-western Tropical Atlantic are among the clearest ocean waters in the world. At the same time, however, it would be problematical to base the optical water type on the results of measurements at only one wavelength. The optical class of water obtained from measurements of $K_d(425)$ was higher (*i.e.* the water was optically clearer) than that found on the basis of $K_d(535)$ values and, moreover, was higher than that obtained using $K_d(\mathrm{PAR})$. The spatial distribution of the optical water type in Figure 5 is the superposition of results in all the above-mentioned spectral bands.

The weak dependence of the colour index on chlorophyll *a* concentration, in comparison with the numerous published results, was, in our opinion, due to the generally low level of chlorophyll concentration in the investigated area.

It is worth adding, that the dependence of the colour index on chlorophyll is much stronger if the data from the whole penetration depth are taken into account.

Disregarding this might be the reason for the slight lowering of chlorophyll concentration in the upper ocean layer computed on the basis of satellite data (Ocean Color, 1989), in comparison with the results presented in this paper.

Acknowledgements

The authors thank Dr Kazimierz Furmańczyk (University of Szczecin) for enabling us to take part in the expedition and for making the spectroalbedometer available. We also express particular appreciation to Ludwik Targoński and Jerzy Preiss for preparing the measuring devices and their help in making the measurements.

References

Bird R. E., Riordan C., 1986, *Simple solar spectral model for direct and diffuse irradiance on horizontal and tilted planes at the earth's surface for cloudless atmospheres,* J. Clim. Appl. Met., 25, 1, 87–97.

Bowden K. F., 1983, *Physical oceanography of coastal waters,* John Wiley & Sons, New York, 302 pp.

Cadée G. C., 1975, *Primary production off the Guyane coast,* Neth. J. Sea Res., 9, 128–143.

Dera J., 1992, *Marine physics,* Elsevier, Amsterdam – Oxford – New York – Tokyo, 516 pp.

Gordon H. R., Clark D. K., 1980, *Remote sensing optical properties of a stratified ocean: an improved interpretation,* Appl. Opt. 19, 20, 3428–3430.

Gordon H. R., McCluney W. R., 1975, *Estimation of the depth of sunlight penetration in the sea for remote sensing,* Appl. Opt., 14, 413–416.

Gordon H. R., Morel A. Y., 1983, *Remote assessment of ocean color for interpretation of satellite visible imagery – a review,* Springer, New York, 114 pp.

Jerlov N. G., 1976, *Marine optics,* Elsevier, Amsterdam – Oxford – New York – Tokyo, 231 pp.

Ocean Color – Availability of the global data set., 1989. EOS, 70, 23, 634–65, 640–61.

Oceanobiologia, 1988, T. I, *Biological structure of the ocean,* PWN, Warszawa, 496 pp., (in Polish).

Raymont J. E. G., 1983, *Plankton and productivity in the Oceans,* LIPP, Moskva, (in Russian).

Robinson I. S., 1985, *Satellite oceanography,* Ellis Horwood Limited, Chichester, 455 pp.

Rodionov W. W., Mashtakov J. L., Artemev W. A., 1986, *Influence of river outflow on the optical characteristics of the open ocean waters,* [In:] *Physical and oceanological investigations in the Tropical Atlantic,* A. S. Monin, V. J. Voytova (eds.), Nauka, Moskva, 32–35, (in Russian).

Rühle E., Zalewski J. (eds.), *The Atlantic Ocean,* PWN, Warszawa, 664 pp., (in Polish).

Sathyendranath S., Platt T., 1989, *Remote sensing of ocean chlorophyll: consequence of nonuniform pigment profile,* Appl. Opt., 28, 3, 490–495.

Schott F. A., Böning C. W., 1991, *The WOCE Model in the Western Equatorial Atlantic: Upper Layer Circulation,* JGR, 96, C4, 6993–7004.

Sümnich K. H., 1987, *Callibration and on-board checking of the satellite spectrometer MKS,* [In:] *Influence of the atmosphere on remote sensing of the sea,* T. 2, 138–152, AN SSSR, AN GDR, AN USSR, Moskva, Berlin, Sevastopol, 138–152 (in Russian).

Terziev F. S., Sobchenko E. A., Belyevich R. R., 1986, *Basic scientific results of oceanological investigations of the GOIN experiment in the Atlantic,* [In:] *Itogi Nauki i Tekhniki, Atmosfera, Okean, Kosmos – programma Razrezy,* T. 7, Moskva, 130–143, (in Russian).

Tukey J. W., 1981, *Exploratory data analysis,* MIR, Moskva, 694 pp., (in Russian).